WAVELET TRANSFORM IN CLASSIFICATION OF BIOMEDICAL IMAGES

A. Procházka* and A. Gavlasová*

* Prague Institute of Chemical Technology / Department of Computing and Control Engineering, Technická 1905, 166 28 Prague 6, Czech Republic

A.Prochazka@ieee.org, Andrea.Gavlasova@vscht.cz

Abstract: Segmentation and texture analysis form a very important topic of the interdisciplinary area of image processing with many different applications. The paper presents selected methods of image features extraction using both Radon and Wavelet transforms to evaluate features invariant to image rotation and translation. Features classification is then achieved by self-organizing neural networks. The paper presents (i) how image preprocessing and enhancement can simplify image segmentation, and (ii) how image segments textures can allow image areas classification. Proposed methods have been verified for simulated structures and then used for analysis of biomedical magnetic resonance images of the brain.

Introduction

Basic problems of digital image processing include image de-noising, enhancement, restoration of its corrupted components [1, 2, 3, 4] and segmentation. An example of this process applied to biomedical image processing is presented in Fig. 1. Problems of image segmentation are presented in the initial part of the paper.

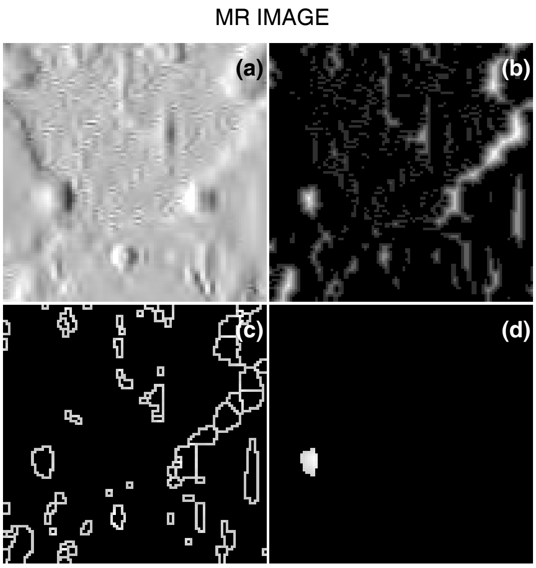

Figure 1: An example of MR image segmentation presenting **(a)** enhanced original MR area, **(b)** distance image transform, **(c)** ridge lines resulting from watershed segmentation, and **(d)** a selected segment

The main part of the paper is devoted to image components analysis and to extraction of their features. In this connection problems of image features invariant to image components rotation and translation are studied using both Radon and Wavelet transforms [5, 6, 7]. Resulting algorithms are verified both for simulated and real magnetic resonance images.

The proposed method is then followed by image components classification and class boundary estimation using self-organizing neural networks.

Image Components Segmentation

Image segmentation methods studied in the paper consist of distance and watershed transform application followed by image ridge lines estimation. Image components features are then evaluated from their boundary signals as well as texture structures.

Segmentation [8, 9] represents an important initial step of image processing. The proposed algorithm consists of these steps

- image thresholding to convert it to the black and white form
- distance and watershed transform use to find image ridge lines presented
- extraction of a segment, its boundary signal and its texture

The process of classification assumes further the definition of a pattern matrix containing features of separate image segments. Many possibilities of their extraction [4] include

- analysis of image boundary signal or the texture inside its area
- analysis of statistical properties of the boundary signal or segment structure
- transform of boundary signal or segment structure allowing its translation and rotation independence using appropriate transforms

Proposed methods of image segmentation have been applied to selected MR images presented in Fig 1 with a chosen boundary signal given in Fig. 2.

Image Features Extraction

To define image features independent to image segments rotation and translation it is useful to apply Radon and

ISSN: 1727-1983

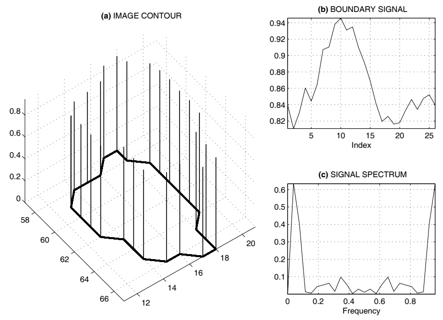

Figure 2: Selected MR image segment analysis showing its boundary signal **(a)** in three and **(b)** in two dimensions followed by **(c)** its discrete Fourier transform

wavelet transforms as the fundamental tools used in the proposed approach [10, 11]. We shall apply this method to a simulated image consisting of segments having the same texture but a different angle of their rotation. Image segments classification is in this case useless as all segments have the same features. Using rotation-invariant texture-analysis technique these features corresponding to individual segments are evaluated and their standard deviation is used as a measure of the efficiency of the proposed method.

Radon Transform

Radon transform forming a very important mathematical tool used in tomography is based upon works of Johann Radon born in 1887 in Litoměřice. His doctoral dissertation has been defended in Vienna in 1910 and his most appreciated works were devoted to integral geometry. The Radon transform [10, 12] belonging to this category introduced in 1917 is defined as a collection of 1D projections around an object at angle intervals Θ. The Radon transform of a two-dimensional (2-D) function $f(x,y)$ is defined as

$$R(\Theta,r)[f(x,y)]=\int_{-\infty}^{+\infty}\int_{-\infty}^{+\infty} f(x,y)\delta(r-x\cos\Theta-y\sin\Theta)\,dx\,dy \tag{1}$$

where r is the perpendicular distance of a line from the origin and Θ is the angle formed by the distance vector. It is possible to analyse this relation taking into account that the value of δ function is nonzero for its argument equal to zero only which means that

$$r-x\cos\Theta-y\sin\Theta \;=\; 0 \tag{2}$$

$$y \;=\; -x\cot\Theta+r/\sin\Theta \tag{3}$$

which for a constant value of Θ represents the set of parallel lines used for the integration of the given image for parameter r. The plane (x,y) is transformed in this way to the plane (Θ,r).

A discrete Radon transform called Hough transform has been introduced in 1972 by R. Duda and P. Hart [13] as a basic tool for image features extraction. Its inverse version forms moreover the fundamental mathematical tool in computer tomography allowing the reconstruction of the two dimensional image from its projections having rotating sources of beams and the set of rotating sensors.

Image Wavelet Decomposition

Signal wavelet decomposition using Discrete Wavelet Transform (DWT) provides an alternative to the Discrete Fourier Transform (DFT) for signal analysis resulting in signal decomposition into two-dimensional functions of time and scale [14]. The main benefit of DWT over DFT is in its multi-resolution time-scale analysis ability.

Wavelet functions used for signal analysis are derived from the initial function $W(t)$ forming basis for the set of functions

$$W_{m,k}(t)=\frac{1}{\sqrt{a}}\,W\,(\frac{1}{a}\,(t-b)) \tag{4}$$

for discrete parameters of dilation $a=2^m$ and translation $b=k\,2^m$. Wavelet dilation, which is closely related to spectrum compression, enables local and global signal analysis. The principle of signal and image decomposition and reconstruction for resolution enhancement is presented in Fig. 3.

The decomposition stage includes the processing of the image matrix by columns at first using wavelet (high-pass) and scaling (low-pass) function followed by row downsampling by factor D in stage $D.1$. To study this problem let us denote a selected column of the image matrix $[g(n,m)]_{N,M}$ as signal $\{x(n)\}_{n=0}^{N-1} = [x(0),x(1),...,x(N-1)]^T$. This signal can be analyzed by a half-band low-pass filter with its impulse response

$$\{s(n)\}_{n=0}^{L-1}=[s(0),s(1),\cdots,s(L-1)] \tag{5}$$

and a complementary high-pass filter having its impulse response

$$\{w(n)\}_{n=0}^{L-1}=[w(0),w(1),\cdots,w(L-1)] \tag{6}$$

The first stage assumes the convolution of a given signal and the appropriate filter for decomposition at first by relations

$$xl(n)=\sum_{k=0}^{L-1} s(k)x(n-k) \qquad xh(n)=\sum_{k=0}^{L-1} w(k)x(n-k) \tag{7}$$

for all values of n followed by subsampling by factor D. In the following decomposition stage $D.2$ the same process is applied to rows of the image matrix followed by row downsampling. The decomposition stage results in this way in four images representing all combinations of low-pass and high-pass initial image matrix processing.

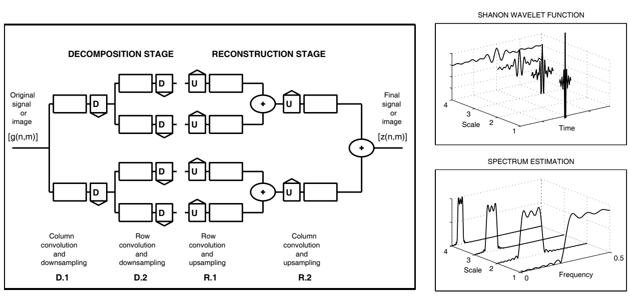

Figure 3: Wavelet transform use in signal decomposition and the effect of Shannon wavelet function dilation to its spectrum compression

ISSN: 1727-1983 © 2005 IFMBE

The reconstruction stage includes row upsampling by factor U at first and row convolution in stage $R.1$. The corresponding images are then summed. The final step $R.2$ assumes column upsampling and convolution with reconstruction filters followed by summation of the results again. In the case of one-dimensional signal processing, steps $D.2$ and $R.1$ are omitted.

Proposed Method

In this section, the rotation-invariant texture-analysis technique using Radon and wavelet transforms is introduced. This technique is depicted in Fig. 4.

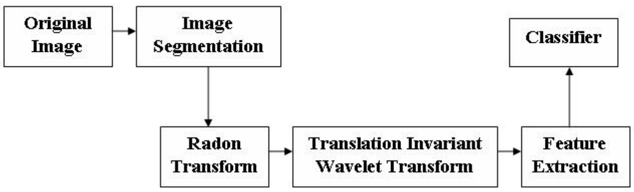

Figure 4: Block diagram of the proposed technique

The illustration shows the procedure of the proposed method in the form of a block diagram. At first all image components are identified using distance and watershed transforms. Then the Radon transform of individual image segments is evaluated followed by the translation-invariant wavelet transform to evaluate its scale components forming basis for the corresponding image segment features. Rotation of the given image corresponds to the translation after the application of the Radon transform along its parameter Θ.

Fig. 5 shows how the Radon transform changes as the simulated image rotates. Figs. 5 (a) and (c) present rotation of the simulated image and its effect to a circular shift along the parameter Θ after the application of the the Radon transform. Therefore, using a translation-invariant wavelet transform along axis Θ, the rotation-invariant features can be estimated.

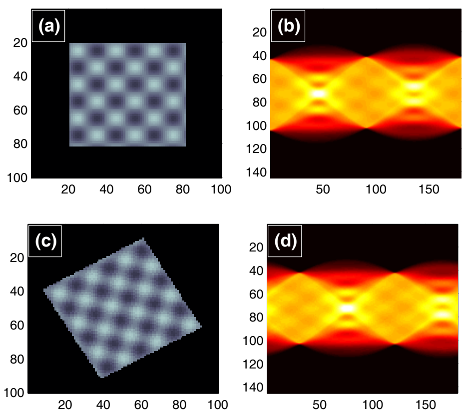

Figure 5: The effect of image rotation to the translation along Θ axis after the application of the Radon transform presenting **(a)** simulated image sample, **(b)** its Radon transform, **(c)** rotated simulated image by angle $\Theta = 30°$, and **(d)** its Radon transform

Results

The main purpose of the paper is to show how the standard deviation of features corresponding to the rotated texture is affected by the use of different methods and combinations of image transforms. The goal is to obtain the same image features independent to image rotation. Fig. 6 presents results of analysis of features belonging to a simulated image which rotates by angle starting from $\Theta = 0°$ to $\Theta = 180°$ with step $\Theta = 10°$. It is possible to distinguish very easily the variance of features and to determine the best method.

Characteristic image features shown in Table 1 are computed as the sum of squared diagonal DWT transform coefficients in the first and the second decomposition levels of the rotated image by angle $\Theta = 10°$ and they are shown in figure as a colored dots. The dots in the figure, presenting features, are evaluated **(a)** by direct application of the wavelet transform (DWT) to the rotated simulated image, **(b)** by the DWT applied to the Radon transform (RT) of the rotated image, and **(c)** by the wavelet transform applied to the Radon transform image of the preprocessed image (Pre). Image preprocessing is performed by the application of the wavelet transform followed by the thresholding. This technique is useful for image denoising, image enhancement or improvement of image resolution.

The proposed method of image features extraction allows the estimation of the rotation invariant image features and moreover it is very flexible as it allows the use of different wavelet functions and different rotation steps in case of the Radon transform. Image preprocessing allows further research devoted to the optimization of wavelet coefficients thresholding to denoise the original image.

Feature values presented in Fig. 6 are normalized to the unit circle to have a better comparison of clusters of image features and to allow their subsequent classification by self-organizing neural networks [15] into the given number of classes.

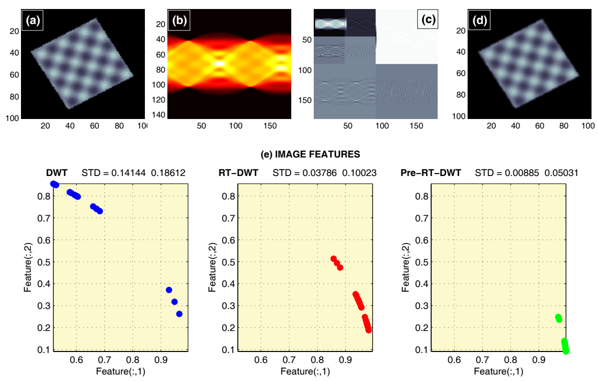

Figure 6: Rotated image features presenting **(a)** rotation of a simulated image, **(b)** its Radon transform, **(c)** decomposition of the Radon transform image into the second level, **(d)** inverse Radon transform of **(b)**, and **(e)** comparison of image features evaluated by methods mentioned in the text

Table 1: Comparison of features evaluated for rotated simulated image presenting in column F1 the sum of squared diagonal DWT coefficients in the first decomposition level and in column F2 the sum of squared coefficients in the second level for 3 different techniques including (i) DWT, (ii) RT-DWT, and (iii) Pre-RT-DWT

Features of Simulated Image						
	DWT		RT-DWT		Pre-RT-DWT	
Angle	F1	F2	F1	F2	F1	F2
0°	0.9284	0.3716	0.8577	0.5141	0.9706	0.2408
10°	0.6029	0.7978	0.9687	0.2482	0.9928	0.1198
20°	0.5278	0.8494	0.9447	0.3280	0.9946	0.1034
30°	0.6021	0.7984	0.9477	0.3192	0.9956	0.0936
40°	0.6595	0.7517	0.9787	0.2053	0.9915	0.1304
50°	0.6724	0.7402	0.9748	0.2230	0.9902	0.1394
60°	0.5994	0.8004	0.9507	0.3102	0.9945	0.1052
70°	0.5193	0.8546	0.9384	0.3455	0.9947	0.1025
80°	0.6050	0.7962	0.9724	0.2334	0.9920	0.1260
90°	0.9482	0.3177	0.8694	0.4940	0.9685	0.2489
100°	0.5770	0.8168	0.9761	0.2172	0.9928	0.1196
110°	0.5179	0.8555	0.9358	0.3524	0.9951	0.0988
120°	0.5935	0.8048	0.9564	0.2920	0.9958	0.0914
130°	0.6706	0.7418	0.9812	0.1929	0.9911	0.1332
140°	0.6827	0.7307	0.9821	0.1882	0.9907	0.1358
150°	0.5822	0.8131	0.9549	0.2970	0.9948	0.1015
160°	0.5264	0.8502	0.9434	0.3316	0.9948	0.1022
170°	0.5765	0.8171	0.9771	0.2129	0.9937	0.1119
180°	0.9650	0.2623	0.8808	0.4734	0.9717	0.2361

Bar plots of rotated image features summarized in Table. 1 are presented in Fig. 7. It is possible to see how the selection of a method affects the variance of evaluated features.

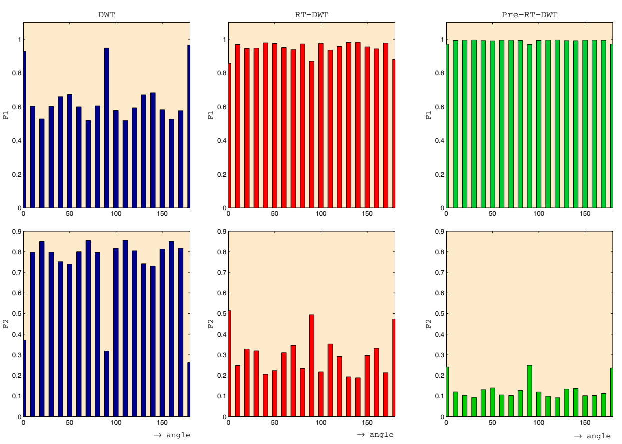

Figure 7: Bar plots of image features evaluated for original texture rotation using proposed methods summarized in Tab. 1

Conclusion

The proposed technique was verified for simulated images and then applied to real MR images. Owing to the difficulty of application of segmentation process we omit this block. Rotation has been applied to the whole MR image segment and features were obtained by the wavelet and Radon transforms and image preprocessing. An example of the rotated MR image and estimated features are presented in Fig. 8.

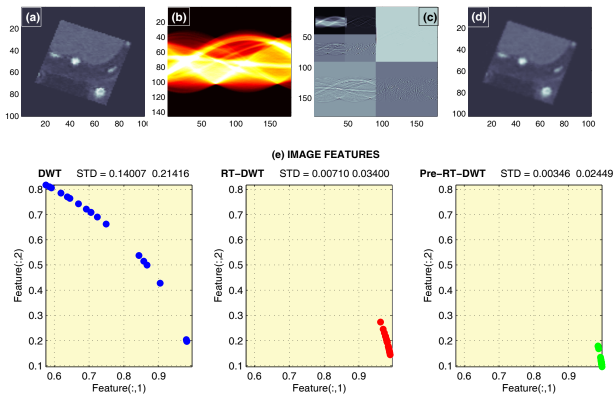

Figure 8: Results of feature extraction methods applied to real MR image processing

Apparently in Fig. 6, 8 the recommended connection of Radon and wavelet transforms dramatically keep down the features variance influenced by image rotation. If we moreover add the image preprocessing results are even better visible. Together with the visual comparison the concrete numerical results obtained point to the efficiency of proposed method as presented in Tables 2 and 3.

Table 2: Comparison of standard deviation (STD) of the sum of squared diagonal DWT transform coefficients in the first and the second decomposition levels using images obtained by rotation from 0 to 180 degrees with step 10° using (i) the plain DWT, (ii) the Radon transform (RT) followed by DWT, and (iii) the RT applied to the preprocessed image (Pre) followed by the DWT

STD of Simulated Image Features		
	Feature-1	Feature-2
DWT	0.1414	0.1861
RT-DWT	0.0379	0.1002
Pre-RT-DWT	0.0089	0.0503

Tables 2 and 3, thanks to the objective confrontation of STDs, are bright examples that the Radon transform is a powerful tool expressively contributing to image analysis. Improvement of STD between the plain DWT and RT-DWT about order has been verificated. We achieved visible improvement by preprocessing of simulated image (Table 2) and a small improvement by denoising of the magnetic resonance image (Table 3). Therefore image enhancement is very desirable here.

Table 3: Comparison of standard deviation (STD) of the sum of squared diagonal DWT transform coefficients in the first and the second decomposition levels using images obtained by rotation from 0 to 180 degrees with step 10° using (i) the plain DWT, (ii) the Radon transform (RT) followed by DWT, and (iii) the RT applied to the preprocessed a image (Pre) followed by the DWT

STD of MR Image Features		
	Feature-1	Feature-2
DWT	0.0013	0.0254
RT-DWT	$2.97 \cdot 10^{-5}$	0.0023
Pre-RT-DWT	$1.4 \cdot 10^{-5}$	0.0016

It is assumed that further studies will be devoted to feature based image segmentation and further methods of rotation and translation invariant feature selection using appropriate image transforms.

Acknowledgments

The work has been supported by the research grant of the Faculty of Chemical Engineering of the Institute of Chemical Technology, Prague No. MSM 6046137306.

References

[1] PROCHÁZKA, A., GAVLASOVÁ, A., VOLKA, K. (2005): 'Wavelet Transform in Image Recognition', In International conference ELMAR05, Zadar. Croatia, IEEE

[2] GULERYUZ, O.G. (2002): Iterated Denoising for Image Recovery, In Data Compression Conference (DCC '02), Snao Bird, Utah, IEEE

[3] STARCK, J.L., CANDES, E., DONOHO, D.L. (2002): The Curvelet Transform for Image Denoising, IEEE Trans. on Image processing, 11(6):670–684

[4] NIXON, M., AGUADO, A. (2004): Feature Extraction & Image Processing, NewNes Elsevier

[5] ARIVAZHAGAN, S., GANESAN, L. (2004): Automatic Target Detection Using Wavelet Transform, Eurasip Journal on Applied Sig. Proc., 17:2663–2674

[6] JAFARI-KHOUZANI, K., SOLTANIAN-ZADEH, H. (2005): Rotation-Invariant Multiresolution Texture Analysis Using Radon and Wavelet Transforms, IEEE Trans. on Image processing, 14(6):783–795

[7] TOFT, P. (1996): The Radon Transform - Theory and Implementation, PhD thesis, Technical University of Denmark

[8] ARIVAZHAGAN, S., GANESAN, L. (2003): Texture Segmentation Using Wavelet Transform, Pattern Recogn. Lett., 24(16):3197–3203

[9] GONZALES, R.C., WOODS, R.E., EDDINS, S.L. (2004): Digital Image Processing Using MATLAB, Prentice Hall

[10] http://en.wikipedia.org/wiki/radon_transform (2005): Internet Encyklopedia, 7, 84.226.54.188

[11] http://www-stat.stanford.edu/~jstarck/ (2005): The Curvelet Home Page

[12] BRACEWELL R.N. (2003): Fourier Analysis and Imaging, Kluwer Academic Press

[13] DUDA, R.O., HART, P.E. (1972): Use of the Hough Transformation to Detect Lines and Curves in Pictures, Comm. ACM, 15(1):11–15

[14] KINGSBURY, N.G. (2001): Complex Wavelets for Shift Invariant Analysis and Filtering of Signals, Journal of Applied and Computational Harmonic Analysis, 10(3):234–253

[15] CHOI, D.I., PARK, S.H. (1994): Self-Creating and Organizing Neural Networks, IEEE Trans. Neural Networks, 5(4):561–575

ISSN: 1727-1983 © 2005 IFMBE